Burrowing behaviour of robotic bivalves with synthetic morphologies

Germann, Daniel P ; Carbajal, Juan Pablo

Abstract: Several bivalve species burrow into sandy sediments to reach their living position. There are many hypotheses concerning the functional morphology of the bivalve shell for burrowing. Observational studies are limited and often qualitative and should be complemented by a synthetic approach mimicking the burrowing process using a robotic emulation. In this paper we present a simple mechatronic set-up to mimic the burrowing behaviour of bivalves. As environment we used water and quartz sand contained in a glass tank. Bivalve shells were mathematically modelled on the computer and then materialized using a 3D printer. The burrowing motion of the shells was induced by two external linear motors. Preliminary experiments did not expose any artefacts introduced to the burrowing process by the set-up. We tested effects of shell size, shape and surface sculpturing on the burrowing performance. Neither the typical bivalve shape nor surface sculpture did have a clear positive effect on burrowing depth in the performed experiments. We argue that the presented method is a valid and promising approach to investigate the functional morphology of bivalve shells and should be improved and extended in future studies. In contrast to the observation of living bivalves, our approach offers complete control over the parameters defining shell morphology and motion pattern. The technical set-up allows the systematic variation of all parameters to quantify their effects. The major drawback of the built set-up was that the reliability and significance of the results was limited by the lack of an optimal technique to standardize the sediment state before experiments.

DOI: https://doi.org/10.1088/1748-3182/8/4/046009

Burrowing behaviour of robotic bivalves with synthetic morphologies

D P Germann[1] and J P Carbajal[2]

[1] Artificial Intelligence Laboratory, Department of Informatics, University of Zürich, Andreasstrasse 15, 8050 Zürich, Switzerland

[2] Department of Electronics and Information Systems, Ghent University, Sint Pietersnieuwstraat 41, 9000 Ghent, Belgium

E-mail: germann@ifi.uzh.ch, juanpablo.carbajal@ugent.be

Abstract. Several bivalve species burrow into sandy sediments to reach their living position. There are many hypotheses concerning the functional morphology of the bivalve shell for burrowing. Observational studies are limited and often qualitative and should be complemented by a synthetic approach mimicking the burrowing process using a robotic emulation. In this paper we present a simple mechatronic set-up to mimic the burrowing behaviour of bivalves. As environment we used water and quartz sand contained in a glass tank. Bivalve shells were mathematically modelled on the computer and then materialized using a 3D printer. The burrowing motion of the shells was induced by two external linear motors. Preliminary experiments did not expose any artefacts introduced to the burrowing process by the set-up. We tested effects of shell size, shape and surface sculpturing on the burrowing performance. Neither the typical bivalve shape nor surface sculpture did have a clear positive effect on burrowing depth in the performed experiments. We argue that the presented method is a valid and promising approach to investigate the functional morphology of bivalve shells and should be improved and extended in future studies. In contrast to the observation of living bivalves, our approach offers complete control over the parameters defining shell morphology and motion pattern. The technical set-up allows the systematic variation of all parameters to quantify their effects. The major drawback of the built set-up was that the reliability and significance of the results was limited by the lack of an optimal technique to standardize the sediment state before experiments.

Keywords: Bivalves, burrowing mechanics, granular media, functional morphology, morphology optimisation

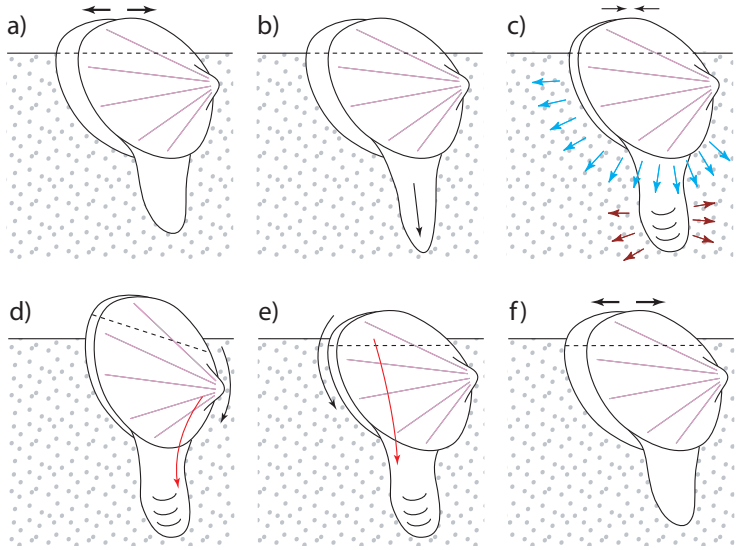

Figure 1: The *burrowing sequence* for bivalves as described by Trueman (1966). (a) The clam is in erect position, partially burrowed in the sediment. The valves are open to anchor the shell, i.e. to prevent back-slippage. (b) The foot probes deeper into the sediment. (c) The adductor muscles contract, partially closing the shell. The water expelled from the cavity liquefies the surrounding sediment to reduce the resistance to penetration. From the soft body inside the shell, blood is pressed into the foot, which is inflated and serves as a new anchor. (d) The anterior retractor muscle (red arrow) pulls the front side of the bivalve towards the foot, leading to a rotation of the shell (black arrow). (e) In the same way, the posterior retractor muscle rotates the shell back into the erect position. (f) The two rotations around different rotation axes led to a net downward translation, as illustrated by the dashed line. The valves open again to allow for another burrowing cycle starting at (a). The figure was inspired by the figure used by Amler et al. (2000, p. 46); reprinted from Koller-Hodac et al. (2010), ©2010 IEEE.

1. Introduction

Bivalve species present a wide variety of modes of life, including lying on the ocean floor, attachment to hard surfaces by their byssus or through cementation, as well as boring and burrowing into soft substrates. There are several reasons for digging into soft substrates: reduction of predation, reduced exposure to sunlight (especially on beaches) and water currents, minimisation of desiccation, and buffering of environmental extremes of temperature, salinity and pH level (Sassa et al., 2011; Watters, 1993).

Bivalves dig into soft sediments using a two-anchor principle as described in figure 1. As anchors they use their shell and a muscular tongue-like expansion of their soft body called *the foot*. The sequential contraction of the anterior and posterior retractor muscles in the foot induces a rocking motion. For *Ensis directus* the retraction force, i.e. the force to pull themselves into the sediment, is known to be up to 10 N (Trueman, 1967).

Bivalves typically dig down to depths 1-3 times their body length (Cox, 1971;

Holland and Dean, 1977; Ziegler, 1983). The time needed to reach the final burrowing depth varies from a few seconds to many minutes (McLachlan et al., 1995; Trueman, 1967; Ziegler, 1983).

Due to the important role of the shell in burrowing, it is believed that its morphology is subject to strong evolutionary pressure. Although it is not entirely clear how the evolutionary process acts on the functional morphology, it seems plausible that there is a need to maximize burrowing speed and the capacity to reach a depth that allows optimal protection (Sassa et al., 2011; Watters, 1993). However, there is also a clear pressure to stay in shallower habitats due to the higher concentration of nutrients (Edelaar, 2000).

The (functional) morphology of bivalve shells can be analysed using different morphometric parameters. The parameter spaces they define are called *morphospaces* (McGhee, 1999). A particular shell morphology can be represented as a point in this space. The *actual* morphospace is constructed by all specimens found in nature, while the *theoretical* morphospace spans all theoretically possible shapes using the given morphometric parameters. In our project we focused on round, inflated shells (*Cardium*, *Venus*) rather than elongated shells (*Ensis*, Winter et al. 2012), because in the former type of bivalve, the rocking motion and shell surface sculpturing are more prominent and therefore the variety of different morphologies and behaviours is greater. While elongated species usually burrow in anterior direction, more compact species may burrow in any direction between anterior and ventral (Kauffman, 1969).

Biological findings are usually achieved by the observation of natural organisms. It is a challenge to quantify aspects of dynamic processes involving living animals. The restriction to existing specimens offers only a sparse representation of the morphological variety and the quantification of their morphological differences is not well-defined, so that generalisations are difficult. In palaeontology, the analysis of bivalve fossils is usually restricted to the shape of the shell and of conserved burrows, and to chemical or physical properties of the sediment. Analyses based on observation of natural specimens can only elucidate the actual morphospace but never the theoretical one.

The synthetic approach to biology, i.e. the construction and analysis of artificial emulations of natural organisms, can help to overcome these difficulties (Pfeifer et al., 2007; Webb, 2000). Due to technical advancements synthetic approaches have recently become more popular and have been successfully applied in fields such as biomimetics, biorobotics and embodied artificial intelligence. It has been widely used to study many different types of locomotion, e.g. legged walking, climbing, undulatory swimming, winged flying, and also locomotion on and within granular media (Jung et al., 2011; Li et al., 2013; Maladen et al., 2011; Mazouchova et al., 2013).

Although there is a large literature about the functional morphology of bivalves, only two examples of application of the synthetic approach to bivalve burrowing are known to the authors, by Stanley (1975, 1977) and Winter et al. (2012).

In his brilliant studies, Stanley produced casts of *Mercenaria mercenaria* (Stanley, 1975) and *Trigoniids* (Stanley, 1977), which he compared to altered copies. In the first case, he tested a shell where the blunt anterior area of *Mercenaria mercenaria*

had been filled up by a more streamlined, sharp cover, in the second case he tested a variant of *Trigonia* with a smooth shell surface instead of the natural sculpture. Stanley reproduced the burrowing process by pushing the cast models into a sandy sediment from above using two rods. In both cases he measured a significant improvement of the natural shapes over the altered ones. He found that the reason were rotation axes shifted outwards to increase the net downward motion. The rocking motion that bivalves use to burrow consists of two rotations induced by the pedal retractors and almost no translation. Neither rotation axis coincides with the centre of gravity of the shell which shows that the shell shape indeed influences the rotational movement. Stanley found that the described morphological features of the tested shells moved the rotation axes further outwards, thus increasing the burrowing efficiency.

A more recent example of a synthetic approach used to study bivalve burrowing is the work by Winter. He identified the fast burrowing bivalve *Ensis directus* as one of the most efficiently burrowing animals (Winter and Hosoi, 2011). He built a robot inspired by this species that used an imitation of the opening and closing valves to fluidize the sediment surrounding the shell and thus reducing the resistance to penetration (Winter et al., 2012). Using this bioinspired technique, the efficiency of previous burrowing and anchoring devices could be greatly improved (Winter and Hosoi, 2011).

Computer simulations often are at the core of the synthetic approach. Sometimes they do not only complement experimental set-ups, but completely replace them. However, it is difficult to computationally simulate bivalve burrowing. While simplified simulations could hardly capture the effects of, e.g., surface sculpture, it would be very labour-intensive to produce a realistic bottom up simulation of the granular media including details such as force chains, fluid-sediment interaction and non-convex grain shapes, even with current state-of-the-art software and algorithms. Therefore, we currently do not see a practicable way to replace a real physical set-up by a simulation for the purpose of studying detailed shell-sediment-water interaction.

In the following, we describe a biomimetic set-up built to apply the synthetic approach to bivalve burrowing. The set-up was designed to mimic the burrowing process using a technical device, that offers new perspectives and ways for the investigation of biological and palaeontological questions, addressing the limitations of observational approaches. After preliminary experiments to test the usability of the set-up, a series of experiments was performed to investigate the effects of cross-sectional area, overall shell shape, sculpture and water expulsion.

2. Materials and Methods

Bivalve burrowing was mimicked using the experimental set-up shown in figure 2a. Bivalve shells were represented by one-piece 3D-printed ABS plastic models. Using a 3D printer, a large variety of different shell morphologies could be tested. The burrowing environment consisted of a tank containing water and quartz sand. The shells were attached to an outside actuation system by two cables that simulated the retractor

muscles of natural bivalves. The set-up did not feature any further representation of the foot. This simplification was done because it would have been technically difficult to build an actuated soft foot of only a few centimetres. Experiments were performed by pulling the artificial shells into the sediment using a rocking motion induced by alternate pulling of the cables. The measurement system was integrated into the control system of the linear motors. A separate system provided a water supply to the shells to simulate water expulsion.

2.1. Shell Models

Bivalve geometries were generated using a method similar to the ones described by Fowler et al. (1992). A planar closed aperture curve was defined using NURBS (non-uniform rational B-splines) and discretized into n points. In $m-1$ discrete growth steps, these points were scaled by a scaling factor and rotated around a fixed axis. The result was a tube-like surface defined by $n \times m$ points. The small end forming the umbo was closed by a simple disc, while the large end forming the aperture and shell edge was closed by a flat disc featuring a structure for easy attachment to the other parts. Using a computer-aided design (CAD) program, this attachment area could be easily adapted to different needs.

The surface sculpture was added in a second step by perturbing the surface in normal direction according to an arbitrary periodic function. We generated shells with radial and commarginal ridges. Using NURBS, it was possible to create ridges with any profile (e.g. jig-saw).

The final closed geometry meshes for the two valves of a shell were printed using a 3D printer. Figure 3 shows the set of shapes that were tested for this study. The layer resolution of the printer was 0.1778 mm; radial ridges converging towards the umbo started to merge at a wavelength of about 0.5 mm. We found that the abrasion of the shells by the sand was negligible (≤ 0.5 mm at the shell front after 280 burrowing runs).

To test generic, simple shapes, we used a circular aperture curve to generate most of the shells shown in figure 3. However, using NURBS, also other shapes could be generated, e.g. the asymmetric shell B-natural. It was also possible to add a translational component along the hinge axis to the coiling of the shell. However, it has to be taken care that whorls of the shell do not separate or overlap in a way that renders the resulting geometry unprintable.

We used a modular approach for the assembly of the shells. The two valves were rigidly fixed to a central stainless steel disc via a bayonet coupling and a locking bolt, as depicted in figures 2b and 4. This mechanism allowed quick replacement of the valves and the minimisation of printer material, since the central part could be reused.

Natural bivalves use their retractor muscles in the foot to pull the shell downwards. Since we had a closed object without mantle cavity, we could not attach the actuating cables inside the shell models. Instead, we used flat rods that protruded from the ventral region of the models to attach the cables, see figure 2b.

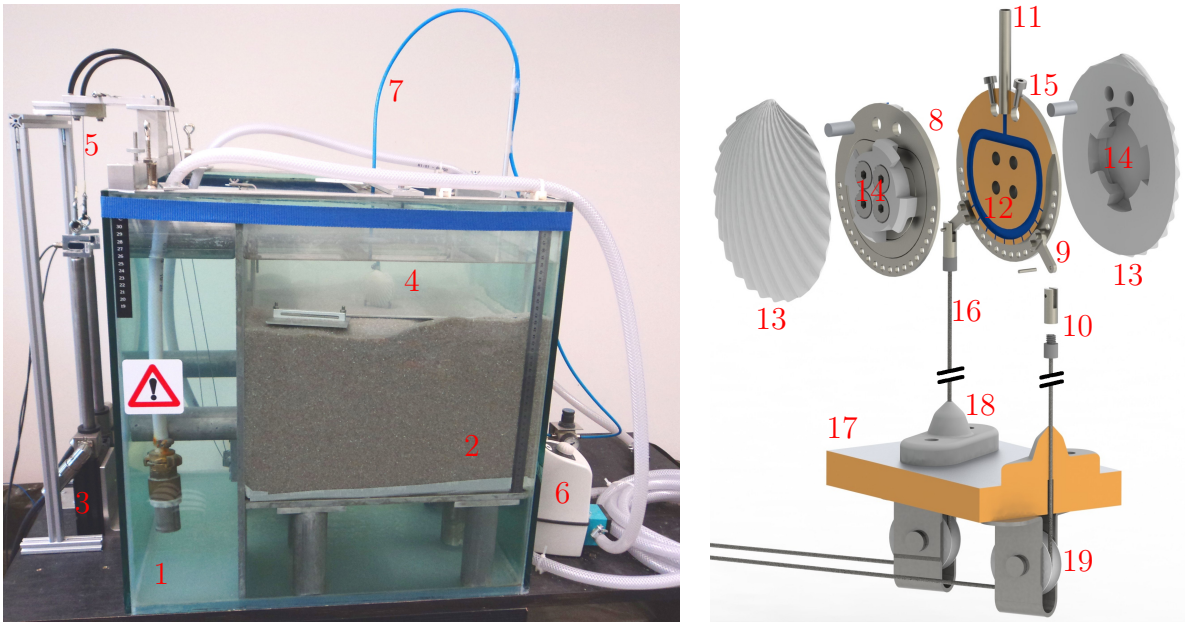

(a) (b)

Figure 2: The experimental set-up used to simulate bivalve burrowing. (a) The experiments were done in a cubic water tank (1) containing a compartment of well-rounded quartz sand (2). Two linear motors (3) vertically mounted on the outside of the tank provided an external actuation of the shell (4). Their force was transmitted by steel cables (5) deviated by pulleys to meet the shell in the sediment from below. The bivalve-like rocking burrowing motion was induced by alternate pulling of the motors. Water for the water ejection was supplied by a pump (6) through a flexible supply tube (7). (b) Details of the modular shell and the cable pulling system: the central part of the shell was a steel disc (8, cut in two halves at the orange area), which was attached to the cables at its cable attachment arms (9). The arms could be fixed at different locations along the lower (ventral) edge of the shell. The shells were attached to the cables by clevises screwed to small cylindrical parts at the end of the cables (10). The flexible supply tube (7) of the water expulsion system was put over a steel duct (11) at the top of the metal disc. From there, the water was pumped through the water expulsion channels (12, blue) out of the shell at the ventral edge. Different valves (13) could be attached to the central disc using a bayonet coupling (14). The valves were locked by bolts (15) fixed by small screws. The cables (16) went through holes in the bottom plate (17, section view, cut at the orange areas). Soft silicone sheaths (18) were used to prevent sand from entering the holes in the bottom plate and abrading the cables. Pulleys (19) were used to deviate the cables and guide them to the linear motors outside the tank.

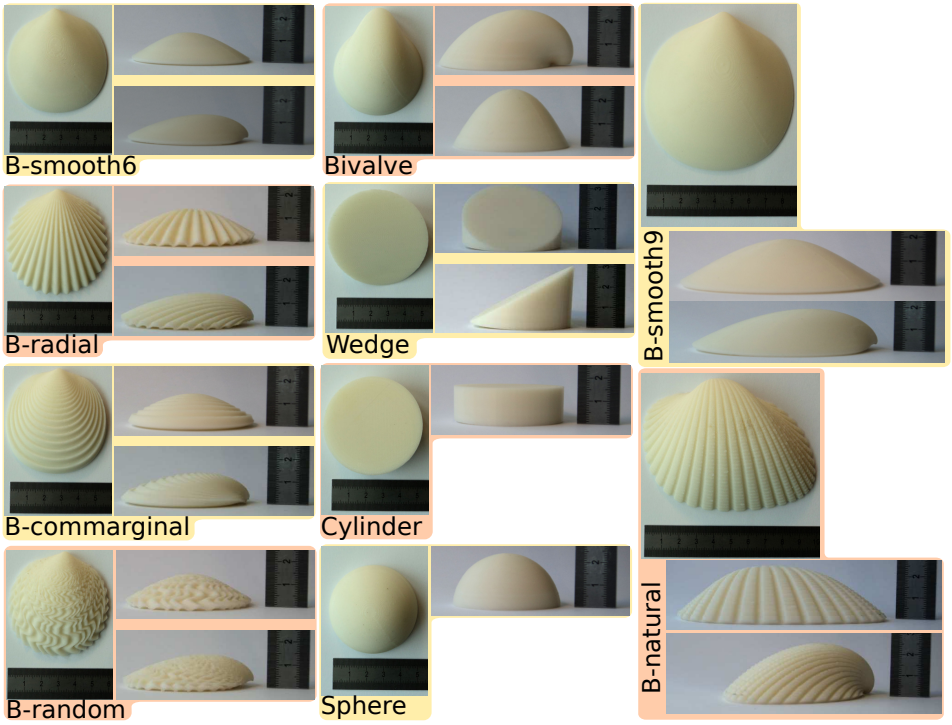

Figure 3: The set of shell shapes used for this study. Only one valve is shown for each. The bivalve-like shapes (starting with "B") were generated using the mathematical model described in section 2.1. Sphere, Cylinder and Wedge were simple geometric shapes of the same volume as Bivalve. The aperture curve of Bivalve was the same circle of 52 mm diameter the three geometric shapes were based on. B-natural was an artificially generated bivalve shape based on the morphology of a bivalve species existing in nature, *Cardium pseudolima*. B-smooth6, B-commarginal, B-radial and B-random did all have the same simple bivalve shape and size, but different sculptures added to their surface: no sculpture, commarginal sculpture (wave length at ventral edge: 5.5 mm, sine-shaped ridge profile), radial sculpture (wave length at ventral edge: 6 mm, terrace shaped ridge profile with the gentle slope towards the burrowing direction), and random sculpture, respectively. The whorl expansion rates (increase in size of the aperture curve after one revolution) are 620 for B-smooth6, B-radial, B-commarginal, B-random and B-smooth9, 30 for B-natural and 12 for Bivalve.

2.2. Water Tank and Sediment

The experiments were done in a cubic water tank (side length 60 cm) containing a compartment (42 ×58 ×24 cm) of well-rounded sorted quartz sand (grain size 0.7 – 1.2 mm, bulk density 1.5 g/cm^3).

To control the initial state of the sediment before each experiment, we manually pressed a small metal plate on the sediment surface to increase its compaction and to undo the loosening caused by retrieving the shell from the previous burrowing run. The height and planarity of the sediment surface was ensured by sliding a metal strip over

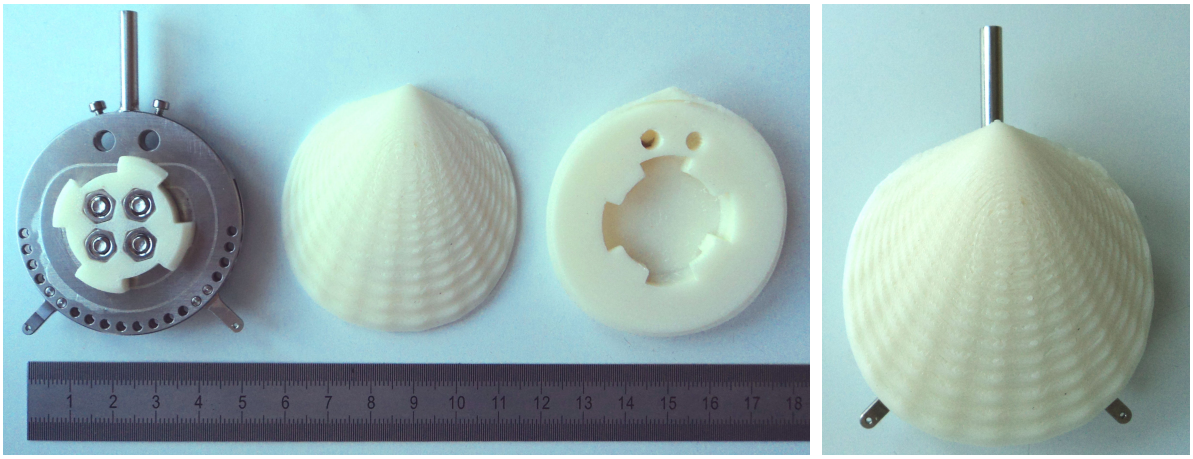

(a) (b)

Figure 4: Modular shell. (a) Central metal disc with male bayonet coupling part, outside of one valve with surface sculpture and inside of the second valve with female coupling part (from left). (b) Assembled shell featuring the cable attachment arms and the water supply duct (cf. figure 2b)

two metal bars horizontally fixed to either side of the sediment compartment. Ensuring a similar state of compaction of the sediment before each experiment was one of the major difficulties of the experiments (see section 4.3).

2.3. Actuation and Measurement System

To transmit the force from the externally mounted linear motors to the shells within the sediment, we used steel cables (Carl Stahl® U 8199512, $8 \times 19 + 7 \times 7$, cable diameter 0.95 mm (steel core) or 1.2 mm (with coating), min. breaking load 850 N). These were each deviated through the set-up using a Bowden cable housing and two pulleys. The cables entered the sediment compartment from below through holes in the aluminium bottom plate. To avoid sand grains from entering the holes and damaging the cables, we added silicone sheaths, see figure 2b.

We used two LinMot® P01-37x240F/460x660-C linear motors with the following characteristics: stroke max.: 660 mm, peak force: 206 N, force constant: 25.8 N/A, max. velocity: 2.6 m/s, position repeatability: ±0.01 mm. B1100-GP-HC controllers provided the proportional-integral-derivative (PID) control of the motors.

For each motor, a force sensor was screwed to the motor slider end and the cable was attached to the sensor. We used ME-Meßsysteme GmbH KD40S sensors with a nominal force range of ±500 N.

At the other end of each cable a screw connector was mounted (see figure 2b). A clevis screwed to the connector added a joint to allow the shell to rotate around a transverse axis and thus perform a rocking motion.

In every experiment, we indirectly measured and recorded the burrowing depth

and retractor pulling forces. To achieve this, the signals from the force sensors and the slider position signals from the linear motor controllers were collected by a National Instruments™ CompactDAQ (data acquisition) device. Because the cables were tight at all times, the burrowing depth could be measured as the displacement of the sliders during the burrowing process.

2.4. Water Expulsion System

Water channels were an additional feature of the central disc (see figure 2b). Their purpose was to allow the ejection of water along the ventral edge to simulate the water expulsion bivalves create when closing their valves.

The pump used for the water supply provided a pressure of 1 bar and a volume flow of 3 l/min. It sucked water from the tank and maintained a constant pressure in a wound up hose from where it could be supplied to the bivalve model through a flexible tube by operating a valve. The valve command signal was generated by one of the controllers of the electrical motors and thus synchronized with the burrowing motion. The amount of water expelled during 500 ms was 15 cm^3. It was therefore comparable to the volumes of the shells ranging from 30 cm^3 (B-smooth6) to 150 cm^3 (B-natural). Water expulsion durations were tested in a realistic range of 0.1 s to 1 s (in nature, durations may go up to several seconds, e.g. in *Mya*, Checa and Cadée 1997).

2.5. Burrowing Motion Control

The open loop control of the actuation system was designed to mimic the rocking burrowing motion of bivalves described in figure 1. The motion pattern was implemented as a sequence of pulling steps as shown in figure 5a, whose timing was similar to the natural case. The measured observables were the tension on the cables f and the displacement of the sliders of the linear motors s. The tension on the cables is a proxy of the force generated in the biological situation by the muscle driving the foot of the bivalve and its interaction with the surrounding sediment. The displacements of the sliders of the linear motors allowed to measure the displacement of the shell within the sediment. In the natural case, this displacement is limited by the maximum length of the foot retractor muscle.

2.6. Experiments

The described set-up was successfully used in a large number of experiments. Figure 3 shows the subset of shell shapes that were tested for this study. For all experiments, the motion pattern and the used pulling force were held constant while the morphology of the shell was changed.

One burrowing process during which the shell moved from its initial position touching the sediment surface to its final position buried in the sediment was called *burrowing run* or *repetition*. An experiment consisted of several repetitions. Between

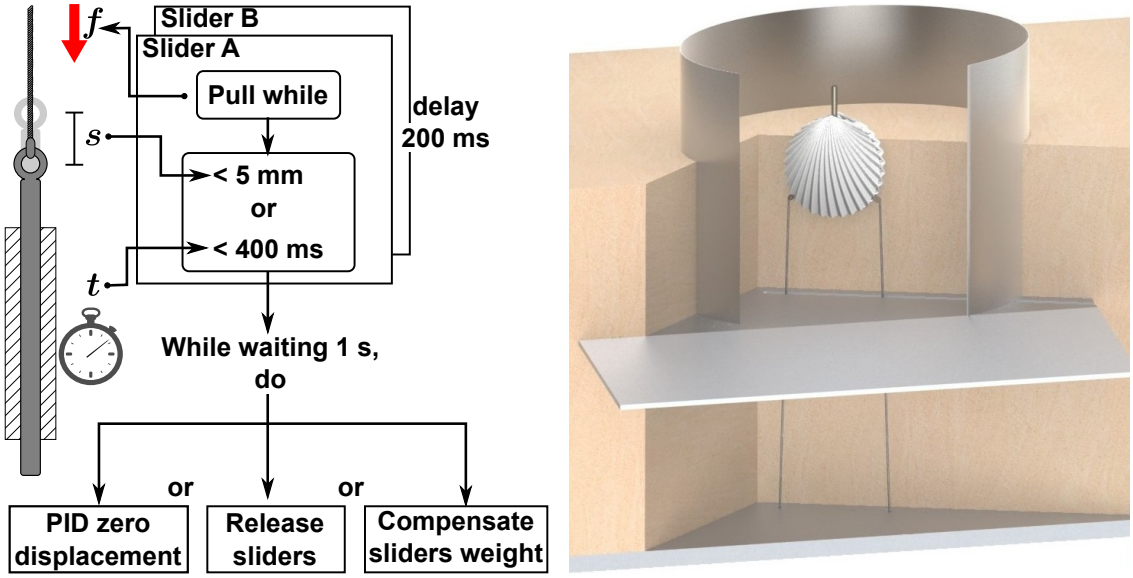

(a) (b)

Figure 5: Artefact testing: (a) Control policy. Scheme of one step of the used control program. A burrowing run consisted of a sequence of such burrowing steps. The second motor connected to the posterior part of the shell executed the same actions as the first motor, delayed by a lag $l = 200$ ms to generate the rocking motion. A constant pulling force f was applied to the motor sliders in the pulling phase. This phase was terminated as soon as either of two conditions was met: 400 ms had elapsed or the sliders had moved over 5 mm. The observed shell displacement values went up to 12.9 mm, the maximum tension observed during our tests was of $f = 200$ N. After a pause of 1 s, the next burrowing step was executed. We tested three different controllers that applied different policies during the pause. The standard controller (1) used PID control to hold the slider position constant during the pause, i.e. to keep the displacement zero. The second controller (2) released the sliders during the pauses, i.e. applied 0 force. The third controller (3) suspended the sliders during the pause by applying a force to compensate for their weight. (b) Sediment confinement. To examine the effect of a confined burrowing area two different cylinder walls (13 cm and 20 cm in diameter) and two different plates (smooth and rough surface) were inserted into the sediment as shown in this cross-sectional view.

experiments, one or several parameters defining shell morphology or motion pattern were changed.

The result plots are based on the measured slider positions, which are denoted as (absolute) burrowing depth. The origin of position was at the sediment surface, with positive values going deeper down into the sediment. The final positions after each burrowing run were averaged between the two motors; repetitions of burrowing runs under identical conditions were summarized by the median of all final burrowing depths. Each box in the depicted boxplots summarizes all repetitions of an experiment.

Final burrowing depth is here defined as the final displacement of the shell, i.e. the distance of the ventral edge to the sediment surface, while in other sources, burrowing depth may mean the distance of the top of the shell to the sediment surface.

The measurements of the slider positions were overestimating the true final burrowing depth due to deformations of the cables and the set-up structure under tension. We measured an increase of $(6.4 \pm 2.2)\%$ (mean $\pm$ standard deviation, $n = 400$) between the depth measured directly by a scale on the water expulsion tube (mean 91.7 mm) and the slider positions (mean 97.6 mm). Since the pulling cables were tight during the burrowing process, the map from the slider positions to the burrowing depth of the shell is monotonic, so that relative comparisons are still valid.

All given p-values are based on a Wilcoxon rank-sum test at a 0.05 significance level to determine the significance of the differences in burrowing depth between different morphologies.

As will be discussed later in section 4.3, there was a memory effect in the sediment that induced a correlation between different experiments. We usually measured a gradual shift of the sediment towards more or sometimes less compaction during the course of a sequence of experiments. Since the sediment standardisation technique described in section 2.2 did not suffice to remove this effect, we did also employ a simple linear model of this drift to alleviate this issue during the evaluation. To this end, the configuration used for the first of a series of experiments was again tested at the end of the series. Because the configurations (i.e. shell morphology and burrowing motion) were identical for the two experiments, their discrepancy provided an estimate of the drift in sediment compaction. By shifting the burrowing depth data of the whole experiment series according to a linear fit through the first and last experiment, the drift could be compensated. Since this procedure modifies the raw data, each of its application is explicitly stated together with the discrepancy of first and last experiment.

2.7. Artefact Testing

Since a new approach to investigate bivalve burrowing was used, several experiments were performed to test the properties of the set-up. Their purpose was to test if the set-up introduced artefacts into the burrowing process that would limit the extent to which the results attained with the set-up can be generalized to other set-ups or to the natural case. Two major aspects were tested, the control policy, i.e. different ways to actuate the shell models, and the sediment confinement, i.e. how a sediment restricted by walls and a bottom plate may be different from an unrestricted, more natural one.

Control policy While in the natural case, bivalves need to anchor their foot to be able to pull themselves deeper into the sediment, the linear motors pulling the shell in our set-up were simply fixed. A natural way to implement the burrowing motion would be to alternately apply a pulling force and no force at all. The control program described in section 2.5 did, instead of applying no force, hold the current position between the

pulling phases. Due to the elasticity of the cables and the set-up structure, the force needed to hold the position increased with burrowing depth. At the point where this holding force reached the magnitude of the pulling force, the shell did not move anymore and the maximal depth was reached. In other words, the linear motors were constantly pulling, with the holding force continuously increasing from 0 to the value of the pulling force. Consequently, the downward motion and the rocking of the shell continuously decreased until they reached 0 at the point where the holding and the pulling forces became equal.

To test if the saturation of the depth curve was an artefact of this set-up dependent effect, we experimented with two alternative controller policies that better reflected the original idea of applying no force between the pulling phases (figure 5a). The first alternative policy did not apply any force between the pulling phases, i.e. completely released the sliders, while the second alternative policy applied a force to compensate the slider weight to set the tension in the cables zero.

Sediment confinement The sediment compartment in the set-up provided only restricted space for the movements of the shell and its surrounding sediment. Objects moving through a granular medium create force chains propagated along touching grains. This effect is called jamming (To et al., 2001; Zhang et al., 2010). In our set-up, sediment jammed against the compartment bottom or walls may have influenced the results of the experiments and explain the saturation behaviour of the depth curve as an artefact of the set-up.

To test the effect of sediment confinement we inserted cylindrical metal walls and horizontal plates into the sediment to change the effective size of the compartment walls (see figure 5b). The two cylindrical walls were of different sizes (13 and 20 cm in diameter). The plates were inserted into the sediment at a depth of 96.4 mm below the sediment surface and provided a 6 mm slit to allow the cables to pass through. To investigate the idea of arcs of sand grains jammed against the bottom plate, we compared the effect of a smooth plate to that of a plate with rough sandpaper attached to its surface. We expected stronger arcs on a rough surface than on a slippery plate. Also, we compared a smooth shell to a radially ridged shell that presumably, together with the rocking motion, would disrupt existing arcs and reduce the jamming effect.

2.8. Basic Shell Morphology Testing

The purpose of the proposed method is to investigate aspects of bivalve burrowing and the functional morphology of bivalve shells. For this study, basic relations were measured: the effect of cross-sectional area of the shell perpendicular to the burrowing direction, and different basic shapes and surface sculptures.

To investigate the influence of shell morphology on the burrowing performance, we separated the shell shape into two levels: overall shape and surface sculpture. The literature suggests that the functional morphology of bivalves has been adapted to

burrowing at both levels (e.g. Alexander et al., 1993; de la Huz et al., 2002; Nel et al., 2001; Savazzi and Huazhang, 1994; Stanley, 1969, 1975, 1977).

Cross-sectional area According to basic soil mechanics, burrowing depth under a given pulling force should inversely correlate with the cross-sectional area of the shell presented to the burrowing direction (Mesri et al., 1996; Sanglerat, 1972). Many bivalves have an elongated shape and burrow with their long axis parallel to the burrowing direction, suggesting that they take advantage of this effect.

To test this basic correlation in our set-up, we analysed burrowing depth measurements from a collection of different experiments using all shells shown in figure 3.

Shell shape To test how bivalve shells compare to other shapes, we measured the performance of four different shapes: a sphere, a disc, a cylinder trunk or wedge-shaped disc, and a bivalve shape ("Sphere", "Cylinder", "Wedge" and "Bivalve" in figure 3). The idea was that the three simple geometric shapes represent different very abstracted versions of bivalve shells. All shapes were smooth, i.e. did not have any sculpture.

All of these shapes had the same volume of 30 cm^3 per valve. This was to make them comparable in an evolutionary sense, i.e. considering the question how evolution would shape the shell given a particular size (volume) of the inner organs of the animal. From a physical point of view, the cross-sectional area perpendicular to the burrowing direction should be kept constant. The pulling force f should be proportional to the density of the sediment ρ, times the gravitational acceleration g, times the cross-sectional area A, times the burrowing depth d (Mesri et al., 1996; Sanglerat, 1972). To compare the experiment results in this respect, we normalized (non-dimensionalized) the measured burrowing depths d by multiplying them with the factor $\rho g A/f$, with $\rho = 1933$ kg/m^3, $g = 9.81$ m/s, $f = 200$ N and using the computed cross-sectional areas that were also used for figure 7.

The same shape may lead to different burrowing depths depending on its orientation. Relative to the umbo and hinge axis of their shell, bivalves burrow in different directions, covering about 90° from ventral to anterior (Kauffman, 1969). To test the effect of different burrowing directions, in addition to the standard experiments in ventral direction, we performed an experiment with B-smooth6, B-radial and B-natural, where the shells were rotated by 90°, such that they entered the sediment in anterior direction.

Surface sculpture To test the effect of surface sculpture, we measured the performance of four shells that had all the same shape and size but different sculpture types added to their surface: radial ridges, commarginal ridges, random ridges (all of the same amplitude) and no sculpture at all. Radial and commarginal ridges are the basic elements of bivalve sculpture and many burrowing species feature either of them or a mixture of both. To separate the effects of sculpturing per se and its

pattern, we also tested a random sculpture with radial ridges sampled from a Gaussian process (Rasmussen and Williams, 2006).

3. Results

In all burrowing experiments, burrowing depth as a function of burrowing time followed a curve similar to the ones shown in figure 6a. It featured discrete staircase-like steps corresponding to the burrowing steps. These steps decreased in size during the course of a burrowing run, i.e. the curve saturated and asymptotically converged to a maximal burrowing depth. All three control policies described in figure 5a exhibited this saturation.

Figure 6b shows the burrowing depth dependent on the different configurations described in figure 5b. The cylindrical walls clearly decreased the burrowing depth, the smaller one by 3.5 cm (37%), the bigger one by 1.6 cm (17%). The plates did not have any clear effect. Although the differences between the configurations using plates are significant, they are only a few millimetres and therefore not clearly distinguishable from fluctuations in the compaction of the sediment. Radial ridges on the shell or sandpaper covering the plate did not introduce major differences either.

Figure 7 shows the depths reached by the different shape models of figure 3. The depth shows roughly a linear relationship with cross-sectional area of the shapes perpendicular to the burrowing direction.

A comparison of the bivalve shell shape Bivalve with the three abstracted shapes Sphere, Wedge and Cylinder is shown in figure 8. Bivalve reached the maximum absolute depth and Cylinder the minimal one, while the other two shapes ranged in between at comparable depths. While the three simple geometric shapes did not protrude out of their ground circle, the umbo of the bivalve shape did, i.e. it was higher than the other three shapes. When considering the relative burrowing depth, i.e. the burrowing depth divided by the shape height, the bivalve shape had a lower performance and ranked even behind the cylinder. In the third plot showing normalized depth, Bivalve has yet another rank, while the ranking of the three other shapes is stable.

For B-smooth6 and B-radial, burrowing in anterior direction led to a depth 2.9 mm lower than when burrowing in ventral direction. For B-natural, the turn towards anterior led to an improvement in burrowing depth of 8.9 mm (see figure 7). However, if again relative depths are computed, the ranking is reversed: B-natural reached a relative depth of 0.69 in the ventral case and of 0.60 in the anterior case. All differences were significant (p-values $\leq 3{\times}10^{-5}$).

Figure 9 shows a comparison between the different tested sculptures. The sculptured shells did not reach larger depths than the smooth shell. Only when comparing normalized depths, B-commarginal had a similar performance as B-smooth6.

We continuously tested the differences between experiments with and without water expulsion. We collected data from 14 pairs of experiments comparing a set-up configuration with and without water expulsion (a total of 175 burrowing runs

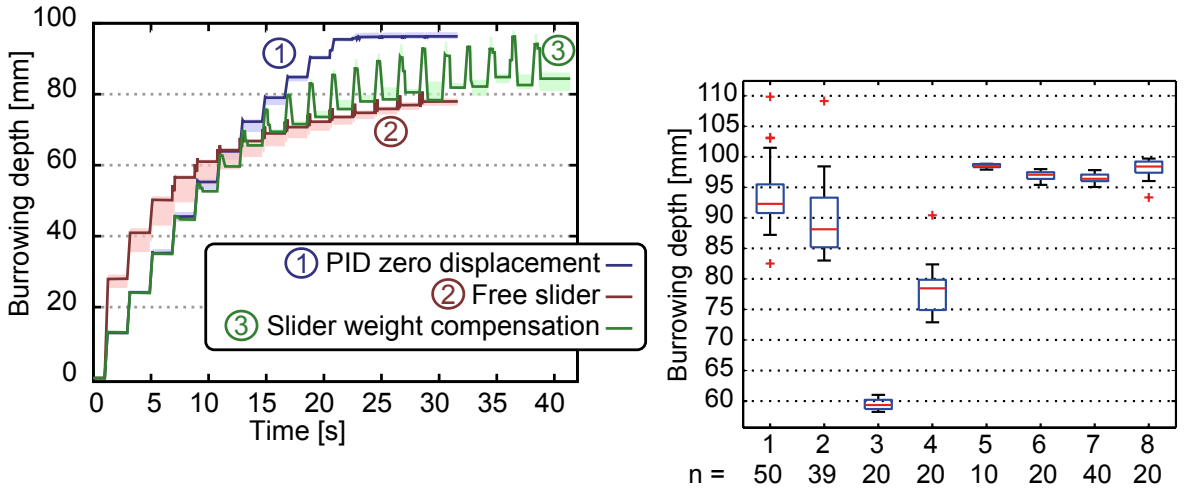

(a) (b)

Figure 6: Artefact testing results. (a) Comparison of the three different controllers (1), (2) and (3) as described in figure 5a. The x-axis shows the experiment (burrowing) time, the y-axis the final burrowing depth reached by the shell. The single burrowing steps are visible as steps in the curves. As the shell penetrates deeper into the sediment the steps gradually diminish, showing a saturation effect for all three controllers. The curves were averaged over 20, 10 and 5 repetitions, respectively. The shaded area contains 100% of the data, the solid line depicts the median. The number of burrowing steps in each experiment was 15, 15 and 20, respectively. The experiments were done using B-smooth6 and identical pulling phases. (b) A boxplot of the results of the confinement tests described in figure 5b. The final burrowing depths are shown for different configurations: (1) B-smooth6, no wall, (2) B-radial, no wall, (3) B-smooth6, small cylindrical wall, (4) B-smooth6, big cylindrical wall, (5) B-smooth6, smooth plate, (6) B-radial, smooth plate, (7) B-smooth6, rough plate, and (8) B-smooth6, rough plate and big cylindrical wall. All other parameters, including the burrowing control were identical. The difference between the experiments 5 and 8 is not significant ($p = 0.91$), the difference between experiments 6 and 7 is barely significant ($p = 0.049$). All other p-values are ≤ 0.003.

each). The used water expulsion duration was 500 ms. We measured a change in burrowing depth of (mean $\pm$ standard deviation) 0.23 ± 2.65 mm or (0.22 ± 2.94)%, i.e. no difference. Only in 7 out of the 14 pairs, the water expulsion led to an improvement.

4. Discussion

The presented set-up was successfully used to perform bivalve burrowing experiments. While shell morphology and burrowing pattern were close to natural bivalves, the necessary pulling force of 200 N is one order of magnitude larger than in the natural case (10 N, *Ensis*). We suspect that this difference is mainly due to dynamic aspects of the natural burrowing process that are missing in our set-up, like a movable soft foot

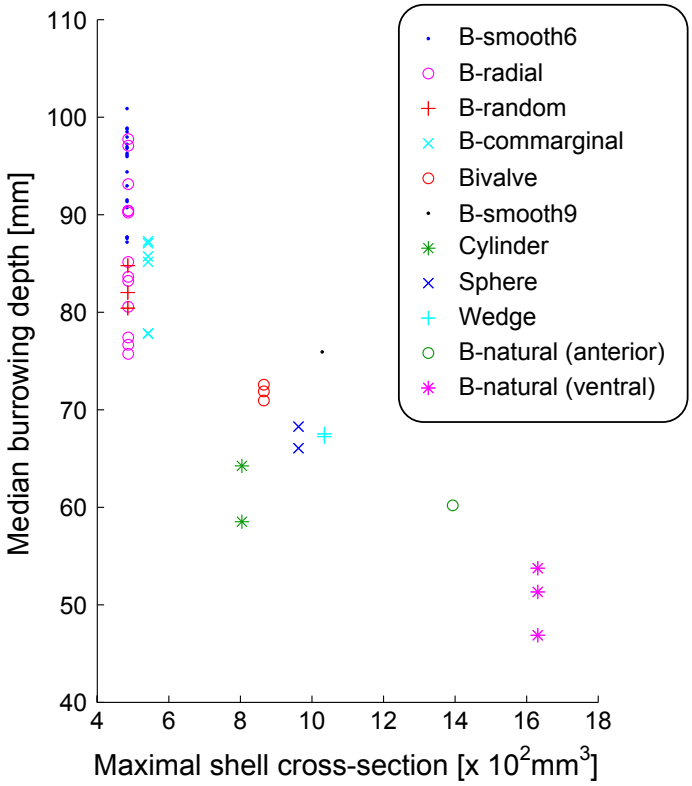

Figure 7: Median burrowing depth dependent on the maximal shell cross section. Every point in this plot shows the result of one of 56 burrowing experiments, each summarising usually 10 repeated burrowing runs (644 burrowing runs in total). All shells shown in figure 3 were evaluated. The x-axis represents the maximum cross-sectional area, perpendicular to the burrowing direction, for one valve of each shell. For B-natural, the results for two burrowing directions are shown, ventral and anterior.

and the opening and closing motion of the valves. However, our simplified set-up allows a systematic analysis of shell morphology and rocking motion.

To our knowledge, Stanley (1975, 1977) was the first and so far only one to manufacture replicas of bivalve shapes to experimentally test how the shell morphology influences the burrowing process. This study builds on his work and tries to expand it in several directions. For instance, by using a pulling mechanism, we were more closely mimicking the foot retractor muscles, and the linear motors could be precisely controlled, while Stanley pushed his models manually or using weights. Also, using computational models of bivalve shell shapes and a 3D printer, a larger number of different shapes can be tested, including artificial shapes, and the experiments are more reproducible, since the shapes are defined exactly. On the other hand, Stanley did an analysis of the rotation axes, which was not possible with the data collected in our experiments (see section 4.4).

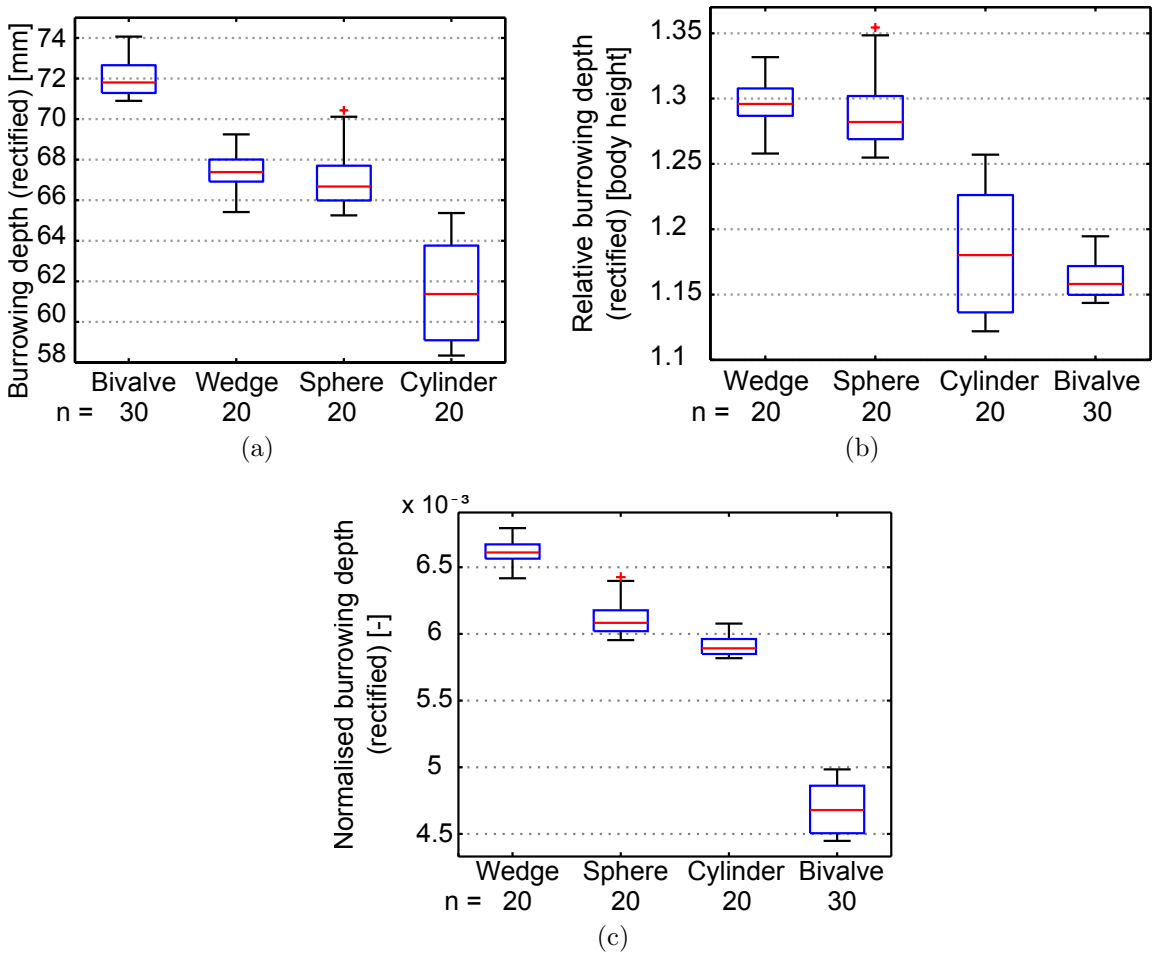

Figure 8: Burrowing depth dependent on shape. The following shell shapes are compared: Bivalve, Sphere, Cylinder and Wedge (cf. figure 3). (a) Absolute burrowing depths. (b) Relative burrowing depths. (c) Normalized burrowing depths (see section 2.8). The data for these plots was linearly shifted; the discrepancy between first and last experiment in this case was 2.5 mm.

4.1. Set-up Artefacts

The set-up was tested for artefacts it may introduce into the experiment results, i.e. effects that reflect the way the set-up works rather than general aspects of bivalve-like burrowing. No significant disturbing effects caused by the motion controllers or by the sediment confinement were found.

Control policies The hypothesis that the saturation behaviour was only due to the increasing position holding forces and therefore an artefact of the set-up was not supported by the data shown in figure 6a. The saturation in the depth curve was present in all control policies suggesting that it was due to the interaction between shell morphology and sediment. The final burrowing depths of the three controllers

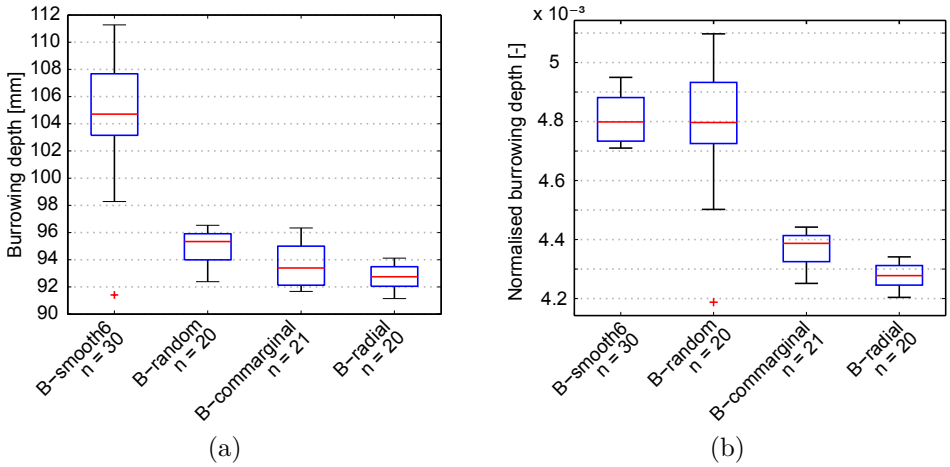

(a) (b)

Figure 9: Burrowing depth dependent on sculpture. The following shell shapes are compared: B-smooth6, B-radial, B-commarginal, B-random, cf. figure 3. (a) Absolute burrowing depths. The difference between B-commarginal and B-radial is not significant ($p = 0.12$). All other differences are significant with $p < 0.0072$. (b) Normalized burrowing depths. The difference between B-commarginal and B-smooth is not significant ($p = 0.92$), all others are significant ($p \leq 3{\times}10^{-5}$).

are consistent with each other. The standard controller (1) reached a depth of almost 100 mm. Controller (2) moved the shell deeper into the sediment in the beginning due to the released sliders that continued pulling by their weight after the actual pulling phase. In the later burrowing phase, the short bursts of the sliders could hardly move the shell anymore. In contrast to the constantly pulling controller (1), the final depth was therefore smaller. The third controller (3) started in a similar way as controller (1), but later oscillated between the final depths of the other two controllers. The reason is that after the pulling phase, the suspended sliders were pulled back up by the tension in the cables and the structure of the set-up. Controller (3) therefore illustrates that the difference between controllers (1) and (2) is due to the motors distorting the set-up rather than a real displacement of the shell in the sediment.

The non-holding controller variants tended to damage the set-up because of the more sudden movements. Since all three controllers led to a saturation process, we consistently used the variant holding the position in all experiments.

Sediment confinement It can be seen immediately from the results in figure 6b that the plates reduced the variance of the measured burrowing depths, but not their absolute values. In the plot, the depth of the plates may be estimated at 100 mm, which deviates by 3.6% from the true value of 96.4 mm. This can be explained by the difference between the slider position and the actual burrowing depth of about 6.4% mentioned earlier.

The cylinder wall of diameter 13 cm decreased the burrowing depth by 3.5 cm and the cylinder wall of diameter 20 cm by 1.6 cm. If fitting a line through these points,

the influence would decrease to zero at a cylinder wall diameter of 26 cm. Even if assuming a very long-tailed curve, the influence of the sediment compartment wall (compartment diameter $\geq$ 42 cm) does not measurably influence the result anymore and should therefore not be distinguishable from an unrestricted sediment.

The results do also show that the sediment was pushed mainly laterally and not downwards. Considering the pulling direction and given that the models used in the experiments did not laterally open the valves, this was unexpected. While we argued above that our sediment compartment was large enough to avoid artefacts due to wall effects, bivalves burrowing in a narrow space between two glass walls may be helpful for the visualisation but not for the investigation of the process.

The results did not show evidence that the radial ridges in connection with the rocking motion or the rough plate influenced the burrowing depth and did therefore not support our hypothesis that these features influence the occurrence or strength of arcs of jammed sand grains. This was unexpected. It seems to follow that jamming is a local effect among the sand grains laterally around the shell.

Another unexpected result was the apparent difference between experiments 4 and 8 (in figure 6b). While the big cylindrical wall clearly reduced the burrowing depth, a plate added to the cylindrical wall removed this effect completely. We cannot offer an explanation for this effect other than a potential error due to the sediment state (see section 4.3).

4.2. Bivalve Burrowing

Burrowing curve In all experiments, a saturation of the burrowing depth in the course of time was measured. While the successive compaction of the sediment may be a general explanation for this, the detailed mechanics are unclear and reducing the phenomenon to a few parameters is not straightforward (cf. paragraph on sculpture below). As we described in the previous section, we did not find artefacts of the set-up influencing the burrowing process. We therefore conclude that the fast convergence to the maximal burrowing depth is an inherent characteristic of the burrowing process and caused by local interactions of shell, water and sand grains.

Cross-sectional area The trend visible in figure 7 is consistent with the basic expectation that larger cross-sectional areas perpendicular to the burrowing direction decrease the burrowing depth. It can, however, be seen that morphology (Cylinder vs. B-smooth9) and sediment fluctuations (B-radial) caused considerable variation in the burrowing depth at fixed values of cross-sectional area. This suggests that by changing their shell shape, bivalves may optimize burrowing depth even if the cross-sectional area is kept constant.

Note that maximum cross-sectional area may change significantly depending on the sculpture details. In particular, B-commarginal may have a larger cross-sectional area than e.g. B-radial, because one of the ridges longitudinally intersects the cross-section.

Shape The results in figure 8 show a stable ranking of Wedge, Sphere and Cylinder, while the performance of Bivalve depends on the measure used. According to these results, a bivalve shape should be more similar to a wedge or a sphere than to a cylinder to increase its burrowing performance. A difference between absolute and relative burrowing depth was also found in the case of burrowing direction. While the absolute burrowing depth of B-natural could be improved by turning it from ventral to anterior and thus reducing the cross-sectional area perpendicular to the burrowing direction, the relative burrowing depth decreased.

Sculpture The results on surface sculpture in figure 9 were unexpected. They suggest that sculpture does not increase burrowing efficiency. If the burrowing depth is normalized by cross-sectional area (figure 9b), B-commarginal performs as well as B-smooth. However, as stated above, maximum cross-sectional area may not be a very stable measure for this type of sculpture.

The results did not support our hypothesis that ridges together with a rocking motion may disrupt jamming in the sediment to increase burrowing depth. Since the literature strongly suggests that sculpture improves the burrowing ability of bivalves (e.g. de la Huz et al., 2002; Savazzi and Huazhang, 1994; Stanley, 1969, 1977), more specific combinations of sculpture (e.g. discordant ridges), burrowing motion and sediment grain size should be tested in future studies. Stanley (1969), e.g., described how ridges rotated into the sediment at a small angle transport grains upwards and the shell downwards.

The results also highlight the difficulty of simulating sculpture-sediment interactions using numerical models, since these models would have to include details at the scale of the sculpture (i.e. three orders of magnitude smaller than the burrowing depth) and of the grain dynamics. Though effective models based on coarse-graining (McComb, 2007; Sahimi, 2003) of granular media dynamics could be suitable to study sculpture-sediment interactions and should be tried, it has been shown that fundamental breakdowns on simple models could render the dynamics not renormalisable (Du et al., 1995; Jaeger et al., 1996) leaving detailed models as the main, if not only, numerical resource to study bivalve burrowing (Herrmann and Luding, 1998; Pöschel and Schwager, 2005).

Water expulsion We did not measure a significant effect of the water expulsion. It is possible that the difficulties with the sediment (see next section) were hiding the (subtle) differences due to the water expulsion. The difficulties with the sediment themselves are a strong argument that bivalves actually do manipulate the sediment state to burrow deeper or faster. We therefore suspect that the explanation for the missing difference is the incomplete representation of water expulsion in our set-up. While our set-up only expels water into the sediment, in the real case, the shells do also close, leading to a volume reduction of the animal and an increased empty space around the shell that can be filled with liquefied sediment.

4.3. Limitations

Synthetic approaches can never capture all aspects of the real process. The focus in the presented set-up lay on the shell morphology and the rocking motion pattern. Depending on the goals of further research, it may be desirable to add more aspects of the natural burrowing process, such as valve motion or an artificial foot or to add a more powerful measurement system (see section 4.4).

A major drawback of the set-up was the lack of an effective method to standardize the state of compaction of the sediment before each experiment. We could not avoid a memory effect, i.e. a dependence of experiments on previous experiments. We measured an approximate compaction state by placing a weighted vertical thin rod on the sediment and observing how far it sank in. The method we applied (section 2.2), did not lead to satisfactory results. However, it was still the most effective method among several tested alternatives. Due to the technical efforts that would have been necessary, we did not implement the mechanism suggested in section 4.4.

The differences between two experiments were often highly significant. However, without satisfactory sediment standardisation, it is difficult to separate the effect of the morphological difference from the effect of the sediment state difference.

We often observed a drift of the state of the sediment to a higher degree of compaction over time. As mentioned in section 2.6, a linear model may be used to remove this drift from the evaluated data. This method was applied to the results shown in figure 8. The number of usually 10 repetitions per experiment was found to be a reasonable compromise between a large sample size for high significance and a compact sequence of experiments where the sediment state did not drift too far away from previous experiments.

Our difficulties with the sediment standardisation are not well reflected in the literature. In his similar study, e.g., Stanley did only mention this issue in one single sentence: “The sediment was packed firmly between experiments.” (Stanley, 1975, p. 53).

In our study, we used burrowing depth as a performance measure. However, as mentioned in the introduction, there is no clear evolutionary pressure for bivalves to maximize burrowing depth. In our experiments, the shells were usually buried to a depth of 0.5 to 1.5 body heights. We may argue that it is a safe assumption that there is an evolutionary pressure to at least cover the whole shell and that we are therefore still in a reasonable range to use depth as a performance measure. Other measures such as burrowing speed or the burrowing rate index (BRI, Stanley 1970) could be used. However, they directly depend on time. Since the temporal pattern of the burrowing process is fixed by the controllers, time cannot be used as a measure. Nevertheless, if a model of the burrowing process was available, other parameters of this model beside the saturation depth could be used. In particular, the change in depth associated with each rocking step (effectively a rate of burrowing) would account for both, maximum depth and speed of burrowing without the explicit use of time measurements.

4.4. Future Work

As possible technical improvements of the set-up we suggest: (1) a better sediment standardisation; based on our experience, we would recommend an automated procedure to first loosen the sediment by pumping in high pressure water and to then vibrate the whole sediment compartment – this should minimize residual structures in the sediment from previous experiments, (2) a more robust structure to be able to test more sudden movements, (3) the automation of the experimentation process (retrieval of the shell, sediment standardisation and initialisation of the shell position and orientation before each experiment), (4) more sensors to gather more detailed information about the burrowing trajectory, and (5) a more sophisticated mechanism for sculpture generation could be used to also test skew and asymmetric sculptures. Also, depending on the goal of future studies, additional aspects of the original process may be implemented, such as movable valves connected by a hinge or an artificial soft foot.

The set-up may then be used to investigate additional shapes, motion patterns and sediment types and to reproduce and expand on the work by Stanley (1975, 1977). In collaboration with biologists and palaeontologists open questions of bivalve functional morphology may be studied and evolutionary experiments may be performed to optimize shell morphology and burrowing motion.

4.5. Conclusion

The synthetic methodology is useful to systematically study the functional morphology of natural processes. In bivalve burrowing and in locomotion through granular media in general, this approach has scarcely been applied. In this paper, we presented a simple mechatronic set-up to mimic the burrowing behaviour of bivalves. Using two linear motors and a system of deviated steel cables, the rocking motion applied by many bivalve species was simulated. We systematically investigated the influence of the shell morphology on the burrowing performance.

We found that the digging motion saturates towards a fixed maximum depth dependent on the morphology. The pressure of the shell against the sediment seems to propagate predominantly in horizontal as opposed to vertical direction, since a cylindrical wall around the burrowing shell reduced the burrowing depth significantly, while a plate inserted into the sediment had almost no influence. It was found that the presented method did not introduce artefacts into the burrowing process.

Using the set-up to test different morphologies, it was found that a wedge is a more efficient burrowing shape than a sphere, which in turn is more efficient than a cylinder. Depending on how the performance is measured, a bivalve shape can have a performance similar to either of the three abstract shapes. In our experiments, sculpture did not increase the burrowing efficiency.

In his study, Stanley (1975, 1977) was restricted in his technical possibilities to test many different morphologies, since he had to manufacture a cast of each shape. He compared a natural shape to an artificially altered version missing a particular

morphological feature (blunt anterior area or surface sculpture). Applying geometrical models and modern 3D manufacturing techniques, in contrast, allows the continuous variation of any modelled parameter and a more precise quantisation of its effect on burrowing performance.

Applying a synthetic approach to study bivalve functional morphology therefore has a large potential. In particular, we see the following advantages: (1) extensive control over the bivalve shell morphology and the applied burrowing motion pattern, (2) the controlled variation of single parameters allows systematic comparisons of morphological traits, (3) effects of shell morphology and burrowing pattern can be easily measured and quantified, (4) no natural shells need to be collected or bought, all shapes can be manufactured by a 3D printer, (5) simplified comparison between shapes because their geometries are well-defined, (6) generation of any shell form, even if it does not exist in nature, i.e. no limitation to the actual morphospace, but potential coverage of the whole theoretical morphospace, (7) shells can be produced in larger quantities; this does not only allow replacing broken shells by another exact copy, increasing the degree of reproducibility, but also gives rise to the possibility of performing evolutionary robotics experiments, (8) 3D printing techniques will be cheaper, faster and more accurate in the future and offer even more possibilities to investigate (functional) morphologies, and (9) there are no ethical issues (as for keeping living bivalves).

Acknowledgments

The authors would like to thank Steven M. Stanley and the people from the MOLLUSCA mailing list for the discussions, Peter Eggenberger Hotz and Wolfgang Schatz for initiating and accompanying this research, Kurt Bösiger from the workshop for his services and Rolf Pfeifer for providing the AILab infrastructure.

We would like to thank the Swiss National Science Foundation [113934, 129900] for funding this project.

Author contributions **DPG** carried out the experiments and data analysis. **JPC** contributed to the experiment design and data analysis. Both authors contributed equally to the writing of this paper.

References

Alexander, R. R., Stanton, R. J. J., and Dodd, J. R. Influence of sediment grain size on the burrowing of bivalves; correlation with distribution and stratigraphic persistence of selected Neogene clams. *Palaios*, 8(3):289–303, 1993.

Amler, M., Fischer, R., and Schröder-Rogalla, N. *Muscheln*, volume 5 of *Haeckel-Bücherei*. Enke im Georg Thieme-Verlag, Stuttgart, 2000. ISBN 3-13-118391-8.

Checa, A. G. and Cadée, G. C. Hydraulic burrowing in the bivalve Mya arenaria linnaeus (Myoidea) and associated ligamental adaptations. *Journal of Molluscan*

Studies, 63(2):157–171, 1997. doi: 10.1093/mollus/63.2.157. URL http://mollus.oxfordjournals.org/content/63/2/157.full.pdf#page=1&view=FitH.

Cox, L. *Mollusca 6: Bivalvia*, volume Part N of *Treatise on invertebrate paleontology*. Geological Society of America, Boulder, Colorado, USA, 1971. ISBN 0-8137-3026-0.

de la Huz, R., Lastra, M., and López, J. The influence of sediment grain size on burrowing, growth and metabolism of Donax trunculus L. (Bivalvia: Donacidae). *Journal of Sea Research*, 47(2):85–95, 2002. ISSN 13851101. doi: 10.1016/S1385-1101(02)00108-9.

Du, Y., Li, H., and Kadanoff, L. P. Breakdown of Hydrodynamics in a One-Dimensional System of Inelastic Particles. *Phys. Rev. Lett.*, 74(8):1268–1271, 1995. doi: 10.1103/PhysRevLett.74.1268. URL http://link.aps.org/doi/10.1103/PhysRevLett.74.1268.

Edelaar, P. Phenotypic plasticity of burrowing depth in the bivalve Macoma balthica: experimental evidence and general implications. *Evolutionary biology of the bivalvia*, 177:451–458, 2000.

Fowler, D. R., Meinhardt, H., and Prusinkiewicz, P. Modeling Seashells. In Catmull, E. E. and McCormick, B. H., editors, *SIGGRAPH '92 conference proceedings*, volume 26.1992,2 of *Computer graphics*, pages 379–387, New York, 1992. ACM Press. ISBN 0201515857.

Herrmann, H. and Luding, S. Modeling granular media on the computer. *Continuum Mechanics and Thermodynamics*, 10(4):189–231, 1998. ISSN 0935-1175. doi: 10.1007/s001610050089. URL http://link.springer.com/10.1007/s001610050089.

Holland, A. F. and Dean, J. M. The biology of the stout razor clam Tagelus plebeius: I. Animal-sediment rlationships, feeding mechanism, and community biology. *Chesapeake Science*, 18(1):58, 1977. ISSN 00093262. doi: 10.2307/1350364.

Jaeger, H., Nagel, S., and Behringer, R. Granular solids, liquids, and gases. *Reviews of Modern Physics*, 68(4):1259–1273, 1996. ISSN 0034-6861. doi: 10.1103/RevModPhys.68.1259. URL http://link.aps.org/doi/10.1103/RevModPhys.68.1259.

Jung, S., Winter, A. G., and Hosoi, A. Dynamics of digging in wet soil. *International Journal of Non-Linear Mechanics*, 46(4):602–606, 2011. ISSN 00207462. doi: 10.1016/j.ijnonlinmec.2010.11.007.

Kauffman, E. G. Form, function, and evolution. In Cox, L. R., editor, *Mollusca 6: Bivalvia*, Treatise on invertebrate paleontology Part N N 0028639. The Geological Society of America, 1969.

Koller-Hodac, A., Germann, D. P., Gilgen, A., Dietrich, K., Hadorn, M., Schatz, W., and Eggenberger Hotz, P. Actuated Bivalve Robot: Study of the Burrowing Locomotion in Sediment. In *IEEE International Conference on Robotics and Automation (ICRA), 2010*, pages 1209–1214, Piscataway, NJ, 2010. IEEE. ISBN 9781424450381.

Li, C., Zhang, T., and Goldman, D. I. A Terradynamics of Legged Locomotion

on Granular Media. *Science*, 339(6126):1408–1412, 2013. ISSN 0036-8075. doi: 10.1126/science.1229163.

Maladen, R. D., Ding, Y., Umbanhowar, P. B., Kamor, A., and Goldman, D. I. Mechanical models of sandfish locomotion reveal principles of high performance subsurface sand-swimming. *Journal of The Royal Society Interface*, 8(62):1332–1345, 2011. ISSN 1742-5689. doi: 10.1098/rsif.2010.0678.

Mazouchova, N., Umbanhowar, P. B., and Goldman, D. I. Flipper-driven terrestrial locomotion of a sea turtle-inspired robot. *Bioinspiration & Biomimetics*, 8(2):026007, 2013. ISSN 1748-3182. doi: 10.1088/1748-3182/8/2/026007.

McComb, W. D. *Renormalization Methods: A Guide For Beginners*. OUP Oxford, 2007. ISBN 9780199236527.

McGhee, G. R. *Theoretical morphology: The concept and its applications*. Perspectives in paleobiology and earth history. Columbia Univ. Press, New York, USA, 1999. ISBN 0231106173.

McLachlan, A., Jaramillo, E., Defeo, O., Dugan, J., Ruyck, and Coetzee, P. Adaptations of bivalves to different beach types. *Journal of Experimental Marine Biology and Ecology*, 187(2):147–160, 1995. ISSN 0022-0981. doi: 10.1016/0022-0981(94)00176-E. URL http://www.sciencedirect.com/science/article/pii/002209819400176E.

Mesri, G., Terzaghi, K., and Peck, R. B. *Soil mechanics in engineering practice*. Wiley, New York, third ed. edition, 1996. ISBN 9780471086581. URL http://sfx.ethz.ch/sfx_locater?sid=ALEPH:EBI01&genre=book&isbn=978-0-471-08658-1.

Nel, R., McLachlan, A., and Winter, D. P. E. The effect of grain size on the burrowing of two Donax species. *Journal of Experimental Marine Biology and Ecology*, 265 (2):219–238, 2001. ISSN 0022-0981. doi: 10.1016/S0022-0981(01)00335-5. URL http://www.sciencedirect.com/science/article/pii/S0022098101003355.

Pfeifer, R., Lungarella, M., and Iida, F. Self-Organization, Embodiment, and Biologically Inspired Robotics. *Science*, 318(5853):1088–1093, 2007. ISSN 0036-8075. doi: 10.1126/science.1145803.

Pöschel, T. and Schwager, T. *Computational Granular Dynamics: Models and Algorithms*. SCIENTIFIC COMPUTATION. Springer, 2005. ISBN 9783540214854.

Rasmussen, C. E. and Williams, C. K. *Gaussian processes for machine learning*. Adaptive computation and machine learning. The MIT Press, Cambridge, 2006. ISBN 978-0-262-18253-9. URL http://www.gaussianprocess.org/gpml/chapters.

Sahimi, M. *Heterogeneous Materials II: Nonlinear and Breakdown Properties and Atomistic Modeling*. Heterogeneous Materials. Springer, 2003. ISBN 9780387001661. URL http://books.google.be/books?id=Fcvxa7UfjgAC.

Sanglerat, G. *The penetrometer and soil exploration: Interpretation of penetration diagrams-theory and practice*, volume 1 of *Developments in geotechnical engineering*. Elsevier, Amsterdam, 1972. ISBN 978-0-444-40976-8.

Sassa, S., Watabe, Y., Yang, S., Kuwae, T., and Thrush, S. Burrowing Criteria and Burrowing Mode Adjustment in Bivalves to Varying Geoenvironmental Conditions in Intertidal Flats and Beaches. *PLoS ONE*, 6(9):e25041, 2011. ISSN 1932-6203. doi: 10.1371/journal.pone.0025041.

Savazzi, E. and Huazhang, P. A. Experiments on the frictional properties of terrace sculptures. *Lethaia*, 27(4):325–336, 1994. ISSN 0024-1164. doi: 10.1111/j.1502-3931.1994.tb01583.x.

Stanley, S. M. Bivalve Mollusk Burrowing Aided by Discordant Shell Ornamentation. *Science*, 166(3905):634–635, 1969. ISSN 0036-8075. doi: 10.1126/science.166.3905.634.

Stanley, S. M. *Relation of shell form to life habits of the Bivalvia (Mollusca)*, volume 125 of *Memoir / The Geological Society of America*. The Geological Society of America, Boulder, Colorado, USA, 1970. ISBN 05854216.

Stanley, S. M. Why Clams have the Shape they Have: An Experimental Analysis of Burrowing. *Paleobiology*, 1(1):48–58, 1975.

Stanley, S. M. Coadaptation in the Trigoniidae, a remarkable family of burrowing bivalves. *Palaeontology*, 20:869–899, 1977.

To, K., Lai, P.-Y., and Pak, H. Jamming of Granular Flow in a Two-Dimensional Hopper. *Physical Review Letters*, 86(1):71–74, 2001. ISSN 0031-9007. doi: 10.1103/PhysRevLett.86.71.

Trueman, E. R. Bivalve Mollusks: Fluid Dynamics of Burrowing. *Science*, 152(3721):523–525, 1966. ISSN 0036-8075. doi: 10.1126/science.152.3721.523.

Trueman, E. R. The dynamics of burrowing in Ensis (bivalvia). *Proceedings of the Royal Society of London. Series B, Biological Sciences*, 166(1005):p 459–476, 1967. ISSN 00804649. URL http://www.jstor.org/stable/75643.

Watters, G. T. Some Aspects of the Functional Morphology of the Shell of Infaunal Bivalves (Mollusca). *Malacologia*, 35(2):315–342, 1993.

Webb, B. What does robotics offer animal behaviour? *Animal Behaviour*, 60(5):545–558, 2000. ISSN 00033472. doi: 10.1006/anbe.2000.1514.

Winter, A. G. and Hosoi, A. E. Identification and Evaluation of the Atlantic Razor Clam (Ensis directus) for Biologically Inspired Subsea Burrowing Systems. *Integrative and Comparative Biology*, 51(1):151–157, 2011. ISSN 1540-7063. doi: 10.1093/icb/icr038.

Winter, A. G., Deits, R. L. H., and Hosoi, A. E. Localized fluidization burrowing mechanics of Ensis directus. *Journal of Experimental Biology*, 215(12):2072–2080, 2012. ISSN 0022-0949. doi: 10.1242/jeb.058172.

Zhang, J., Majmudar, T. S., Sperl, M., and Behringer, R. P. Jamming for a 2D granular material. *Soft Matter*, 6(13):2982, 2010. ISSN 1744-683X. doi: 10.1039/c000147c.

Ziegler, B. *Spezielle Paläontologie: Protisten, Spongien und Coelenteraten, Mollusken*, volume 2/3 of *Einführung in die Paläobiologie / Bernhard Ziegler*. Schweizerbart'sche Verlagsbuchhandlung, Stuttgart, 1 edition, 1983. ISBN 3-510-65036-0.